Electronic Supplementary Material (ESI) for Physical Chemistry Chemical Physics.
This journal is © the Owner Societies 2021

PCCP. **2020.** *Electronic Supporting Materials*

Determination of the dispersion forces in the gas phase structures of ionic liquids using exclusively thermodynamic methods

Dzmitry H. Zaitsau,[a,b] Ralf Ludwig,[a,b,c] Sergey P. Verevkin,[a,b]

[a] Universität Rostock, Institut für Chemie, Abteilung für Physikalische Chemie, Dr.-Lorenz-Weg 2, 18059, Rostock, Germany

[b] Department LL&M, University of Rostock, Albert-Einstein-Str. 25, 18059, Rostock, Germany

[c] Leibniz-Institut für Katalyse an der Universität Rostock e.V., Albert-Einstein-Str. 29a, 18059 Rostock, Germany

Quartz Crystal Microbalance (QCM): Vapor pressures and molar enthalpies of vaporization of ILs, were measured by using the QCM method.[1] A sample of an IL was placed in an open cavity (Langmuir evaporation) inside of the thermostat block and it was exposed to vacuum (10^{-5} Pa) with the whole open surface of the loaded compound. The QCM-sensor was mounted directly above the measuring cavity containing the sample. Along the vaporization into high vacuum, a certain amount of sample was condensed on the quartz crystal surface. The change of the vibrational frequency Δf was recorded. It is directly related to the mass deposition Δm on the QCM according to the Sauerbrey equation:[2]

$$\Delta f = - C \times f^2 \times \Delta m \times S_C^{-1} \quad \text{(S1)}$$

where f is the fundamental frequency of the crystal (6 MHz in this case) with $\Delta f << f$, S_C is the surface of the crystal, and C is a constant.[2] The measured frequency change rates ($df/d\tau$) can be used for calculation of absolute vapor pressures p_s according to equation:

$$p_s = K' \frac{df}{dt} \sqrt{\frac{T}{M}}. \quad \text{(S2)}$$

where the $K' = (9.5 \pm 1.1) \cdot 10^{-6}$ Pa·s·kg$^{1/2}$·Hz^{-1}·K$^{-1/2}$·mol$^{-1/2}$ is the empirical calibration constant including all parameters involved in Eq. 1, as well as the all apparatus geometry specific parameters.[3] Calibration of the set up was performed with the help of reliable vapor pressure data on [C_nPy][NTf_2], [$C_nC_n$im][NTf_2], and [$C_n$mim][NTf_2] series of ionic liquids. Standard molar enthalpy of vaporization, $\Delta_l^g H_m^o(T_0)$, was calculated as follows:

$$\ln\left(\frac{df}{dt}\sqrt{T}\right) = A' - \frac{\Delta_l^g H_m^o(T_0) - \Delta_l^g C_{p_m}^o T_0}{R}\left(\frac{1}{T} - \frac{1}{T_0}\right) + \frac{\Delta_l^g C_{p_m}^o}{R}\ln\left(\frac{T}{T_0}\right) \quad \text{(S3)}$$

where T_0 is an arbitrarily chosen reference temperature (T_0 average temperature of experimental range of the QCM study) and A' is the empirical constant. The value $\Delta_l^g C_{p,m}^o = C_{p,m}^o(g) - C_{p,m}^o(l)$ is the difference between the molar heat capacities of the gaseous $C_{p,m}^o(g)$ and the liquid phase $C_{p,m}^o(l)$ respectively. The vaporization enthalpy $\Delta_l^g H_m^o$ (T) at any temperature is calculated according to Kirchhoff´s equation:

$$\Delta_l^g H_m^o(T) = \Delta_l^g H_m^o(T_0) + \Delta_l^g C_{p,m}^o (T - T_0) \quad \text{(S4)}$$

A typical experiment was performed in a few consequent series with increasing and decreasing temperature steps. Every series included from 7 to 11 temperature points of mass loss rate determination. Such a procedure allowed for detection of any possible decomposition during frequency loss rate (df/dτ) measurements. Reproducibility of results was established in series of randomly performed experimental runs. The study was considered as completed when the $\Delta_l^g H_m^o(T)$-values derived from the temperature-dependent rates (df/dτ) achieved the level of uncertainty of ± 1 kJ·mol^{-1}. Primary experimental results of the QCM studies are provided in Table S1. The absence of decomposition of IL under experimental conditions was controlled by using spectroscopy. The residual amount of IL in the cavity, as well as the IL-deposit on QCM were analyzed by ATR-IR spectroscopy. No changes in the spectra have been detected, as can be seen in Figures S2 to S6.

1 - quartz crystal microbalance (QCM) with the external thermoregulation.
2 – cavity with sample of ionic liquid (measuring cell)
3 - thermostating block.
4 - thermometer
5 - heating ring
6 - cold trap filled with the liquid nitrogen
7 - connection to the turbo molecular pump
8 – Quartz Crystal Monitor Q-Pod by Inficon

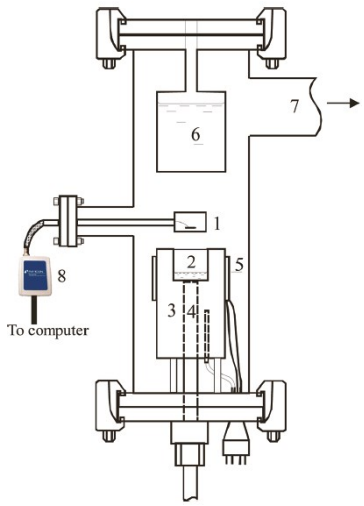

Fig. S1 The scheme of the QCM experimental setup from Ref 1.

Table S1 Results for frequency shifts of quartz, vapor pressure temperature dependence and vaporization enthalpies $\Delta_l^g H_m^o(T)$ determined by QCM for studied ionic liquids.

Run	T / K	$df \cdot dt^{-1}$ / Hz·s^{-1}	$10^6 \cdot p^*_{sat}$ / Pa	T^{-1} / K^{-1}	$R \cdot \ln(p^*_{sat}/p^o)$	$\Delta_l^g H_m^o(T)$ / kJ · mol^{-1}
			[N_{1123}][NTf_2]			
	$\ln\left(p^*_{sat}/p^o\right) = -\frac{76226}{R} - \frac{132411}{R}\left(\frac{1}{T} - \frac{1}{T_0}\right) - \frac{74}{R}\left(\frac{T_0}{T} - 1 - \ln\left(\frac{T}{T_0}\right)\right)$, T_0 = 408.2 K					
1	432.40	0.4976	156	0.002313	-168.6	130.6
	427.40	0.3208	100	0.002340	-172.3	131.0
	422.40	0.2079	64	0.002367	-176.0	131.4
	417.40	0.1340	41	0.002396	-179.7	131.7
	412.40	0.08542	26	0.002425	-183.4	132.1
	407.44	0.05388	16	0.002454	-187.3	132.5
	402.47	0.03358	10	0.002485	-191.3	132.8
	397.49	0.02035	6.1	0.002516	-195.5	133.2
	392.53	0.01212	3.6	0.002548	-199.9	133.6
	387.56	0.007430	2.2	0.002580	-204.0	133.9
2	429.89	0.3992	125	0.002326	-170.5	130.8
	424.91	0.2592	81	0.002353	-174.1	131.2
	419.92	0.1672	52	0.002381	-177.8	131.5
	414.95	0.1075	33	0.002410	-181.5	131.9
	409.99	0.06851	21	0.002439	-185.3	132.3
	405.03	0.04296	13	0.002469	-189.2	132.6
	400.09	0.02651	8.0	0.002499	-193.3	133.0
	395.12	0.01617	4.9	0.002531	-197.5	133.4
	390.15	0.009746	2.9	0.002563	-201.7	133.7
	385.15	0.005542	1.6	0.002596	-206.5	134.1
			[N_{1114}][NTf_2]			
	$\ln\left(p^*_{sat}/p^o\right) = -\frac{76543}{R} - \frac{135535}{R}\left(\frac{1}{T} - \frac{1}{T_0}\right) - \frac{74}{R}\left(\frac{T_0}{T} - 1 - \ln\left(\frac{T}{T_0}\right)\right)$, T_0 = 408.4 K					
1	432.76	0.4774	150	0.002311	-168.9	133.7
	427.77	0.3120	97	0.002338	-172.5	134.1
	422.79	0.2039	63	0.002365	-176.1	134.5
	417.80	0.1312	40	0.002393	-179.8	134.8
	412.79	0.08267	25	0.002423	-183.7	135.2
	407.80	0.05101	16	0.002452	-187.8	135.6
	402.79	0.03041	9.2	0.002483	-192.1	136.0
	397.81	0.01833	5.5	0.002514	-196.4	136.3
	392.82	0.01094	3.3	0.002546	-200.7	136.7
	387.83	0.006403	1.9	0.002578	-205.2	137.1
2	382.85	0.003814	1.1	0.002612	-209.6	137.4

	430.30	0.3857	121	0.002324	-170.7	133.9
	425.28	0.2507	78	0.002351	-174.4	134.3
	420.28	0.1615	50	0.002379	-178.1	134.7
	415.29	0.10222	31	0.002408	-181.9	135.0
	410.31	0.06425	20	0.002437	-185.8	135.4
	405.31	0.03987	12	0.002467	-189.9	135.8
	400.31	0.02394	7.2	0.002498	-194.1	136.1
	395.31	0.01426	4.3	0.002530	-198.5	136.5
	390.31	0.008476	2.5	0.002562	-202.9	136.9
$[N_{1115}][NTf_2]$ $\ln\left(p_{sat}^{*}/p^{o}\right) = -\frac{76420}{R} - \frac{136095}{R}\left(\frac{1}{T} - \frac{1}{T_0}\right) - \frac{83}{R}\left(\frac{T_0}{T} - 1 - \ln\left(\frac{T}{T_0}\right)\right)$, $T_0 = 413.7$ K						
1	442.78	0.9718	303	0.002258	-163.1	133.7
	437.76	0.6459	200	0.002284	-166.5	134.1
	432.75	0.4321	133	0.002311	-169.9	134.5
	427.72	0.2779	85	0.002338	-173.6	134.9
	422.70	0.1734	53	0.002366	-177.6	135.3
	417.68	0.1072	32	0.002394	-181.7	135.8
	412.66	0.06666	20	0.002423	-185.7	136.2
	407.64	0.04160	12	0.002453	-189.6	136.6
	402.62	0.02490	7.4	0.002484	-193.9	137.0
	397.61	0.01550	4.6	0.002515	-197.9	137.4
2	432.74	0.4025	124	0.002311	-170.5	134.5
	427.73	0.2583	79	0.002338	-174.2	134.9
	422.69	0.1673	51	0.002366	-177.9	135.3
	417.67	0.1053	32	0.002394	-181.8	135.8
	412.65	0.06614	20	0.002423	-185.7	136.2
	407.64	0.04143	12	0.002453	-189.7	136.6
	402.62	0.02556	7.6	0.002484	-193.7	137.0
	397.60	0.01505	4.5	0.002515	-198.2	137.4
	392.58	0.009146	2.7	0.002547	-202.4	137.8
	385.56	0.004340	1.3	0.002594	-208.6	138.4
3	435.24	0.4940	153	0.002298	-168.8	134.3
	430.23	0.3250	100	0.002324	-172.3	134.7
	425.21	0.2113	65	0.002352	-175.9	135.1
	420.18	0.1383	42	0.002380	-179.5	135.6
	415.16	0.08596	26	0.002409	-183.5	136.0
	410.14	0.05386	16	0.002438	-187.4	136.4
	405.12	0.03273	9.8	0.002468	-191.6	136.8
	400.10	0.01877	5.6	0.002499	-196.3	137.2
	395.08	0.01173	3.5	0.002531	-200.3	137.6
	389.07	0.006139	1.8	0.002570	-205.7	138.1
$[N_{1224}][NTf_2]$						

$$\ln\left(p^*_{sat}/p^o\right) = -\frac{76355}{R} - \frac{137655}{R}\left(\frac{1}{T} - \frac{1}{T_0}\right) - \frac{91}{R}\left(\frac{T_0}{T} - 1 - \ln\left(\frac{T}{T_0}\right)\right),\ T_0 = 405.0\ \text{K}$$

1	427.73	0.4157	125	0.002338	-170.4	135.6
	417.67	0.1623	48	0.002394	-178.3	136.5
	412.66	0.1017	30	0.002423	-182.3	137.0
	407.64	0.0616	18	0.002453	-186.5	137.4
	402.63	0.03911	11	0.002484	-190.3	137.9
	397.60	0.02230	6.5	0.002515	-195.0	138.3
	392.59	0.01343	3.9	0.002547	-199.3	138.8
	387.58	0.00793	2.3	0.002580	-203.8	139.2
	382.57	0.00448	1.3	0.002614	-208.5	139.7
2	430.25	0.516846	156	0.002324	-168.6	135.4
	425.23	0.3272	98	0.002352	-172.4	135.8
	420.20	0.2055	61	0.002380	-176.4	136.3
	415.18	0.1262	37	0.002409	-180.5	136.7
	410.15	0.0791	23	0.002438	-184.4	137.2
	405.14	0.04875	14	0.002468	-188.5	137.6
	400.12	0.02938	8.6	0.002499	-192.7	138.1
	395.10	0.01754	5.1	0.002531	-197.1	138.6
	390.09	0.01021	2.9	0.002564	-201.6	139.0
	385.08	0.005916	1.7	0.002597	-206.2	139.5

[N_{2225}][NTf_2]

$$\ln\left(p^*_{sat}/p^o\right) = -\frac{75651}{R} - \frac{138075}{R}\left(\frac{1}{T} - \frac{1}{T_0}\right) - \frac{108}{R}\left(\frac{T_0}{T} - 1 - \ln\left(\frac{T}{T_0}\right)\right),\ T_0 = 408.9\ \text{K}$$

1	432.75	0.7118	209	0.002311	-166.2	135.5
	427.73	0.4376	128	0.002338	-170.3	136.0
	422.70	0.2726	79	0.002366	-174.2	136.6
	417.69	0.1727	50	0.002394	-178.1	137.1
	412.66	0.1086	31	0.002423	-182.0	137.7
	407.65	0.06860	20	0.002453	-185.9	138.2
	402.63	0.03934	11	0.002484	-190.5	138.8
	397.62	0.02468	7.0	0.002515	-194.5	139.3
	392.60	0.01446	4.0	0.002547	-199.0	139.8
	387.59	0.008278	2.3	0.002580	-203.7	140.4
2	430.23	0.5539	162	0.002324	-168.3	135.8
	425.21	0.3410	99	0.002352	-172.4	136.3
	420.20	0.2225	64	0.002380	-176.0	136.9
	410.16	0.08555	24	0.002438	-184.0	137.9
	405.14	0.05171	15	0.002468	-188.2	138.5
	395.11	0.01821	5	0.002531	-197.0	139.6
	390.09	0.01100	3.1	0.002564	-201.3	140.1
3	430.22	0.5610	164	0.002324	-168.2	135.8
	425.20	0.3455	101	0.002352	-172.3	136.3

	420.18	0.2156	62	0.002380	-176.2	136.9
	415.16	0.1357	39	0.002409	-180.1	137.4
	410.14	0.08432	24	0.002438	-184.1	137.9
	405.14	0.05277	15	0.002468	-188.1	138.5
	400.12	0.03056	8.6	0.002499	-192.7	139.0
	395.11	0.01904	5.3	0.002531	-196.7	139.6
	390.10	0.01056	2.9	0.002563	-201.6	140.1
	385.10	0.006403	1.8	0.002597	-205.8	140.6
$[N_{1444}][NTf_2]$ $\ln\left(p^*_{sat}/p^o\right) = -\frac{74533}{R} - \frac{139272}{R}\left(\frac{1}{T} - \frac{1}{T_0}\right) - \frac{125}{R}\left(\frac{T_0}{T} - 1 - \ln\left(\frac{T}{T_0}\right)\right)$, $T_0 = 400.2$ K						
	419.86	0.4762	134	0.002382	-169.9	136.8
	414.90	0.2983	83	0.002410	-173.8	137.4
	409.92	0.1793	50	0.002440	-178.1	138.1
	404.96	0.1092	30	0.002469	-182.3	138.7
1	400.01	0.06585	18	0.002500	-186.5	139.3
	395.05	0.03948	11	0.002531	-190.8	139.9
	390.09	0.02323	6.3	0.002564	-195.3	140.5
	380.14	0.007666	2.0	0.002631	-204.6	141.8
	417.35	0.3722	104	0.002396	-172.0	137.1
	412.36	0.2310	64	0.002425	-176.0	137.8
	407.39	0.1374	38	0.002455	-180.3	138.4
	402.43	0.08412	23	0.002485	-184.5	139.0
2	397.52	0.05093	14	0.002516	-188.7	139.6
	392.61	0.03035	8.2	0.002547	-193.1	140.2
	387.66	0.01764	4.8	0.002580	-197.6	140.8
	377.72	0.005774	1.5	0.002647	-207.0	142.1
$[N_{2228}][NTf_2]$ $\ln\left(p^*_{sat}/p^o\right) = -\frac{78972}{R} - \frac{1414351}{R}\left(\frac{1}{T} - \frac{1}{T_0}\right) - \frac{133}{R}\left(\frac{T_0}{T} - 1 - \ln\left(\frac{T}{T_0}\right)\right)$, $T_0 = 413.7$ K						
	435.24	0.2995	84	0.002298	-173.7	138.5
	430.22	0.1850	52	0.002324	-177.8	139.2
	425.21	0.1161	32	0.002352	-181.7	139.8
	420.18	0.07180	20	0.002380	-185.7	140.5
	415.15	0.04399	12	0.002409	-189.9	141.2
1	410.14	0.02668	7.3	0.002438	-194.1	141.8
	405.12	0.01614	4.4	0.002468	-198.3	142.5
	400.11	0.009729	2.6	0.002499	-202.6	143.2
	395.09	0.005675	1.5	0.002531	-207.1	143.8
	390.07	0.003345	0.89	0.002564	-211.5	144.5
	437.80	0.3669	104	0.002284	-172.0	138.1
	432.77	0.2299	65	0.002311	-175.9	138.8
2	427.75	0.1475	41	0.002338	-179.7	139.5
	422.73	0.0914	25	0.002366	-183.7	140.1

	417.71	0.05585	15	0.002394	-187.8	140.8
	412.70	0.03370	9.2	0.002423	-192.1	141.5
	407.68	0.02117	5.8	0.002453	-196.0	142.1
	402.67	0.01274	3.5	0.002483	-200.3	142.8
	397.66	0.007756	2.1	0.002515	-204.5	143.5
	435.26	0.2916	82	0.002297	-173.9	138.5
	430.23	0.1811	51	0.002324	-177.9	139.2
	425.21	0.1150	32	0.002352	-181.8	139.8
	420.19	0.07057	20	0.002380	-185.9	140.5
3	415.16	0.04379	12	0.002409	-189.9	141.2
	410.14	0.02804	7.7	0.002438	-193.7	141.8
	405.12	0.01628	4.4	0.002468	-198.2	142.5
	398.60	0.008070	2.2	0.002509	-204.1	143.4
	395.09	0.005682	1.5	0.002531	-207.1	143.8
	390.08	0.003360	0.90	0.002564	-211.5	144.5

$[N_{2666}][NTf_2]$

$$\ln\left(p_{sat}^{*}/p^{o}\right) = -\frac{77633}{R} - \frac{152156}{R}\left(\frac{1}{T} - \frac{1}{T_0}\right) - \frac{184}{R}\left(\frac{T_0}{T} - 1 - \ln\left(\frac{T}{T_0}\right)\right), \; T_0 = 409.7 \text{ K}$$

	433.22	0.5755	150	0.002308	-169.0	147.8
	428.19	0.3331	86	0.002335	-173.5	148.7
	423.19	0.2022	52	0.002363	-177.8	149.7
1	418.19	0.1222	31	0.002391	-182.0	150.6
	413.19	0.07304	19	0.002420	-186.3	151.5
	408.20	0.04159	10	0.002450	-191.0	152.4
	403.21	0.02390	6.0	0.002480	-195.7	153.3
	425.66	0.2543	66	0.002349	-175.8	149.2
	420.62	0.1523	39	0.002377	-180.1	150.1
	415.63	0.09237	24	0.002406	-184.3	151.1
	410.63	0.05434	14	0.002435	-188.8	152.0
2	405.63	0.03202	8	0.002465	-193.2	152.9
	400.63	0.01857	4.6	0.002496	-197.8	153.8
	395.64	0.01053	2.6	0.002528	-202.6	154.7
	390.66	0.005709	1.4	0.002560	-207.7	155.7
	385.67	0.003220	0.79	0.002593	-212.6	156.6
	428.20	0.3368	87.0	0.002335	-173.5	148.7
	423.18	0.2018	51.8	0.002363	-177.8	149.7
	418.18	0.1223	31.2	0.002391	-182.0	150.6
	413.20	0.07198	18.3	0.002420	-186.4	151.5
3	408.20	0.04242	11	0.002450	-190.9	152.4
	403.21	0.02460	6.2	0.002480	-195.5	153.3
	398.22	0.01395	3.5	0.002511	-200.2	154.3
	393.22	0.007562	1.9	0.002543	-205.4	155.2
	388.24	0.004264	1.0	0.002576	-210.2	156.1

$[N_{2666}][NTf_2]$

$$\ln\left(p_{sat}^{*}/p^{o}\right) = -\frac{77633}{R} - \frac{152156}{R}\left(\frac{1}{T} - \frac{1}{T_0}\right) - \frac{184}{R}\left(\frac{T_0}{T} - 1 - \ln\left(\frac{T}{T_0}\right)\right),\ T_0 = 409.7\ \text{K}$$

	433.22	0.5755	150	0.002308	-169.0	147.8
	428.19	0.3331	86	0.002335	-173.5	148.7
	423.19	0.2022	52	0.002363	-177.8	149.7
1	418.19	0.1222	31	0.002391	-182.0	150.6
	413.19	0.07304	19	0.002420	-186.3	151.5
	408.20	0.04159	10	0.002450	-191.0	152.4
	403.21	0.02390	6.0	0.002480	-195.7	153.3
	425.66	0.2543	66	0.002349	-175.8	149.2
	420.62	0.1523	39	0.002377	-180.1	150.1
	415.63	0.09237	24	0.002406	-184.3	151.1
	410.63	0.05434	14	0.002435	-188.8	152.0
2	405.63	0.03202	8	0.002465	-193.2	152.9
	400.63	0.01857	4.6	0.002496	-197.8	153.8
	395.64	0.01053	2.6	0.002528	-202.6	154.7
	390.66	0.005709	1.4	0.002560	-207.7	155.7
	385.67	0.003220	0.79	0.002593	-212.6	156.6
	428.20	0.3368	87.0	0.002335	-173.5	148.7
	423.18	0.2018	51.8	0.002363	-177.8	149.7
	418.18	0.1223	31.2	0.002391	-182.0	150.6
	413.20	0.07198	18.3	0.002420	-186.4	151.5
3	408.20	0.04242	11	0.002450	-190.9	152.4
	403.21	0.02460	6.2	0.002480	-195.5	153.3
	398.22	0.01395	3.5	0.002511	-200.2	154.3
	393.22	0.007562	1.9	0.002543	-205.4	155.2
	388.24	0.004264	1.0	0.002576	-210.2	156.1

$[N_{6666}][NTf_2]$

$$\ln\left(p_{sat}^{*}/p^{o}\right) = -\frac{77011}{R} - \frac{159011}{R}\left(\frac{1}{T} - \frac{1}{T_0}\right) - \frac{218}{R}\left(\frac{T_0}{T} - 1 - \ln\left(\frac{T}{T_0}\right)\right),\ T_0 = 405.6\ \text{K}$$

	422.85	0.3404	83	0.002365	-173.8	155.3
	417.84	0.1908	46	0.002393	-178.7	156.3
	412.83	0.1119	27	0.002422	-183.2	157.4
	407.82	0.06232	15	0.002452	-188.1	158.5
1	402.80	0.03584	8.6	0.002483	-192.7	159.6
	397.79	0.01948	4.6	0.002514	-197.8	160.7
	392.79	0.01081	2.6	0.002546	-202.8	161.8
	387.77	0.005962	1.4	0.002579	-207.8	162.9
	382.76	0.003122	0.73	0.002613	-213.2	164.0
	425.35	0.4483	110	0.002351	-171.5	154.7
2	415.30	0.1460	35	0.002408	-180.9	156.9
	410.34	0.08430	20	0.002437	-185.5	158.0
	405.32	0.04768	11	0.002467	-190.3	159.1

	400.32	0.02654	6.3	0.002498	-195.2	160.2
	395.31	0.01505	3.6	0.002530	-200.0	161.3
	390.30	0.008055	1.9	0.002562	-205.3	162.3
3	422.86	0.3457	85	0.002365	-173.7	155.3
	417.85	0.1934	47	0.002393	-178.6	156.3
	412.84	0.1126	27	0.002422	-183.1	157.4
	407.84	0.06485	16	0.002452	-187.7	158.5
	402.83	0.03533	8.5	0.002482	-192.8	159.6
	397.82	0.01986	4.7	0.002514	-197.7	160.7
	392.81	0.01105	2.6	0.002546	-202.6	161.8
4	425.31	0.4450	109	0.002351	-171.6	154.7
	420.31	0.2532	62	0.002379	-176.3	155.8
	415.28	0.1464	36	0.002408	-180.9	156.9
	410.27	0.08285	20	0.002437	-185.7	158.0
	405.26	0.04771	11	0.002468	-190.3	159.1
	400.25	0.02724	6.5	0.002498	-195.0	160.2
	395.24	0.01475	3.5	0.002530	-200.2	161.3
	390.22	0.007785	1.8	0.002563	-205.6	162.4
$\ln\left(p^*_{\mathrm{sat}}/p^{\mathrm{o}}\right) = -\frac{80977}{R} - \frac{162375}{R}\left(\frac{1}{T} - \frac{1}{T_0}\right) - \frac{228}{R}\left(\frac{T_0}{T} - 1 - \ln\left(\frac{T}{T_0}\right)\right)$, $T_0 = 428.2$ K			[N_{1888}][NTf_2]			
1	452.50	0.6012	151	0.002210	-168.9	156.9
	447.49	0.3646	91	0.002235	-173.1	158.0
	442.47	0.2326	58	0.002260	-176.9	159.2
	437.48	0.1413	35	0.002286	-181.1	160.3
	432.48	0.08496	21	0.002312	-185.3	161.4
	427.48	0.04998	12	0.002339	-189.8	162.5
	422.48	0.02895	7.0	0.002367	-194.4	163.7
	417.50	0.01649	4.0	0.002395	-199.1	164.8
	412.51	0.009459	2.3	0.002424	-203.8	165.9
	407.53	0.005411	1.3	0.002454	-208.5	167.1
2	449.98	0.4574	114	0.002222	-171.2	157.5
	444.99	0.2967	74	0.002247	-174.8	158.6
	439.97	0.1802	45	0.002273	-179.0	159.7
	434.95	0.1085	27	0.002299	-183.3	160.9
	429.93	0.06442	16	0.002326	-187.7	162.0
	424.92	0.03783	9.2	0.002353	-192.1	163.1
	419.90	0.02158	5.2	0.002381	-196.9	164.3
	414.89	0.01245	3.0	0.002410	-201.5	165.4
	409.88	0.007030	1.7	0.002440	-206.3	166.5
	404.88	0.004041	0.96	0.002470	-210.9	167.7

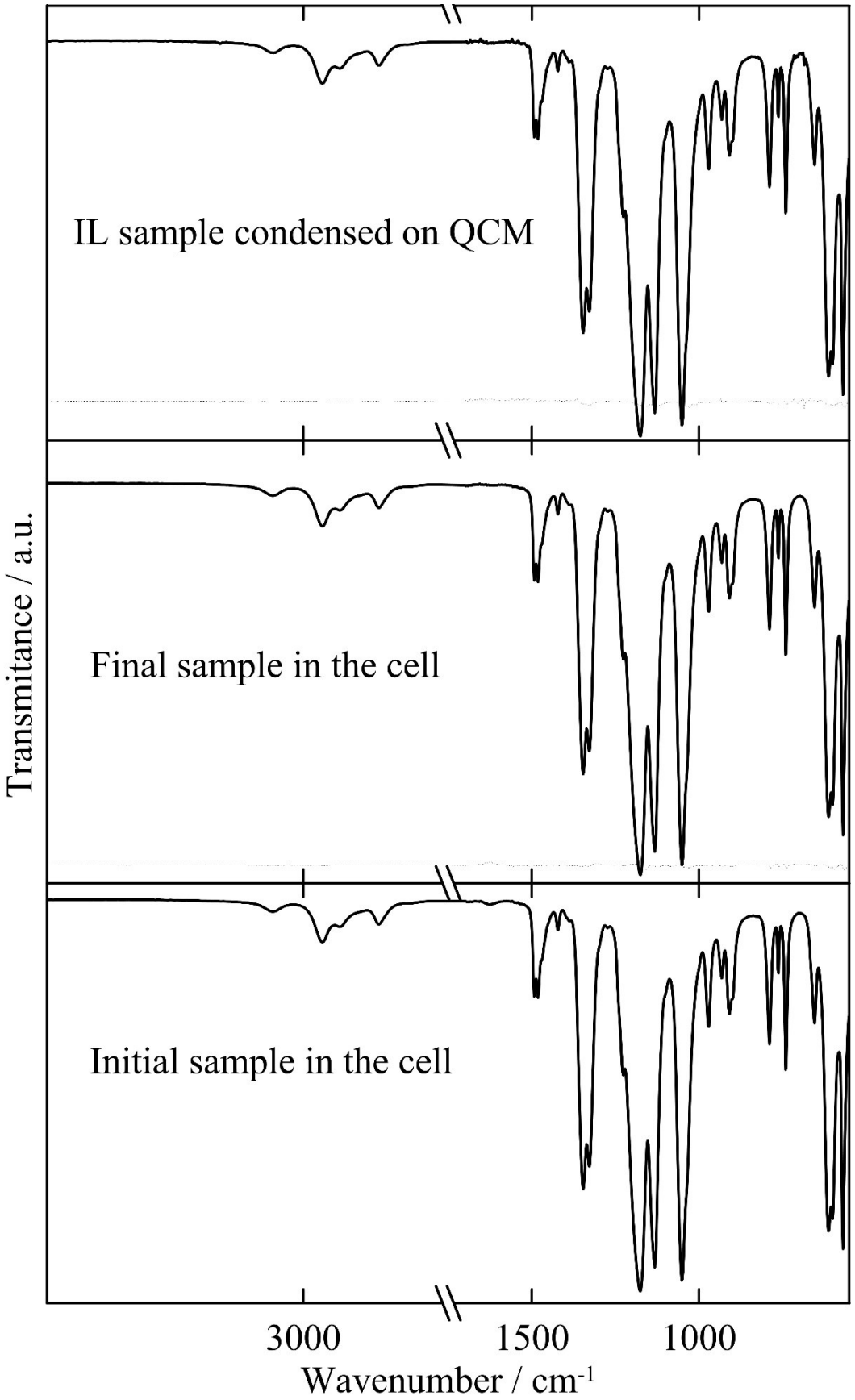

Fig. S2 The spectra of $[N_{1114}][NTf_2]$ studied with QCM technique. Dotted line corresponds to changes in spectra in comparison to initial sample.

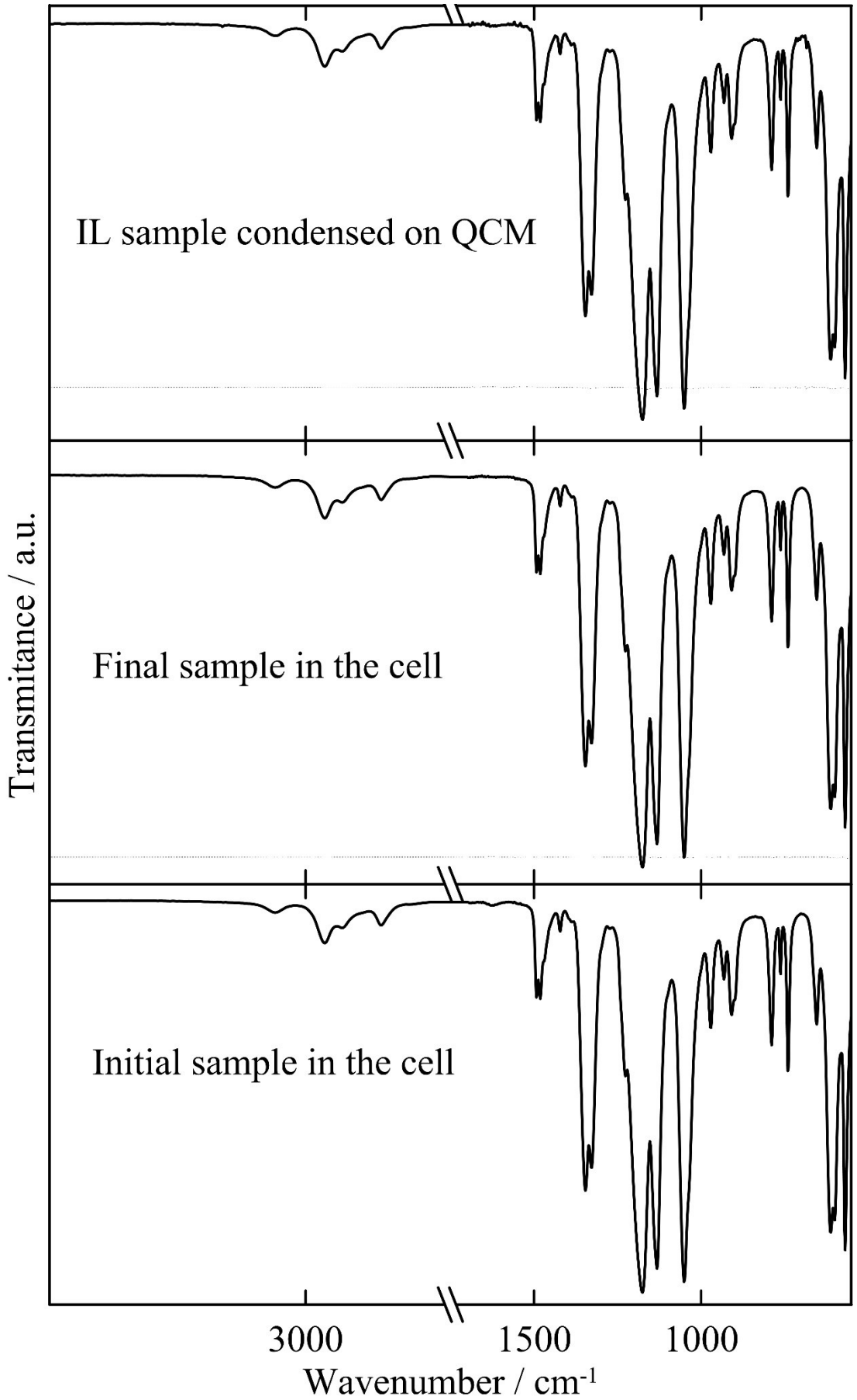

Fig. S3 The spectra of $[N_{1115}][NTf_2]$ studied with QCM technique. Dotted line corresponds to changes in spectra in comparison to initial sample.

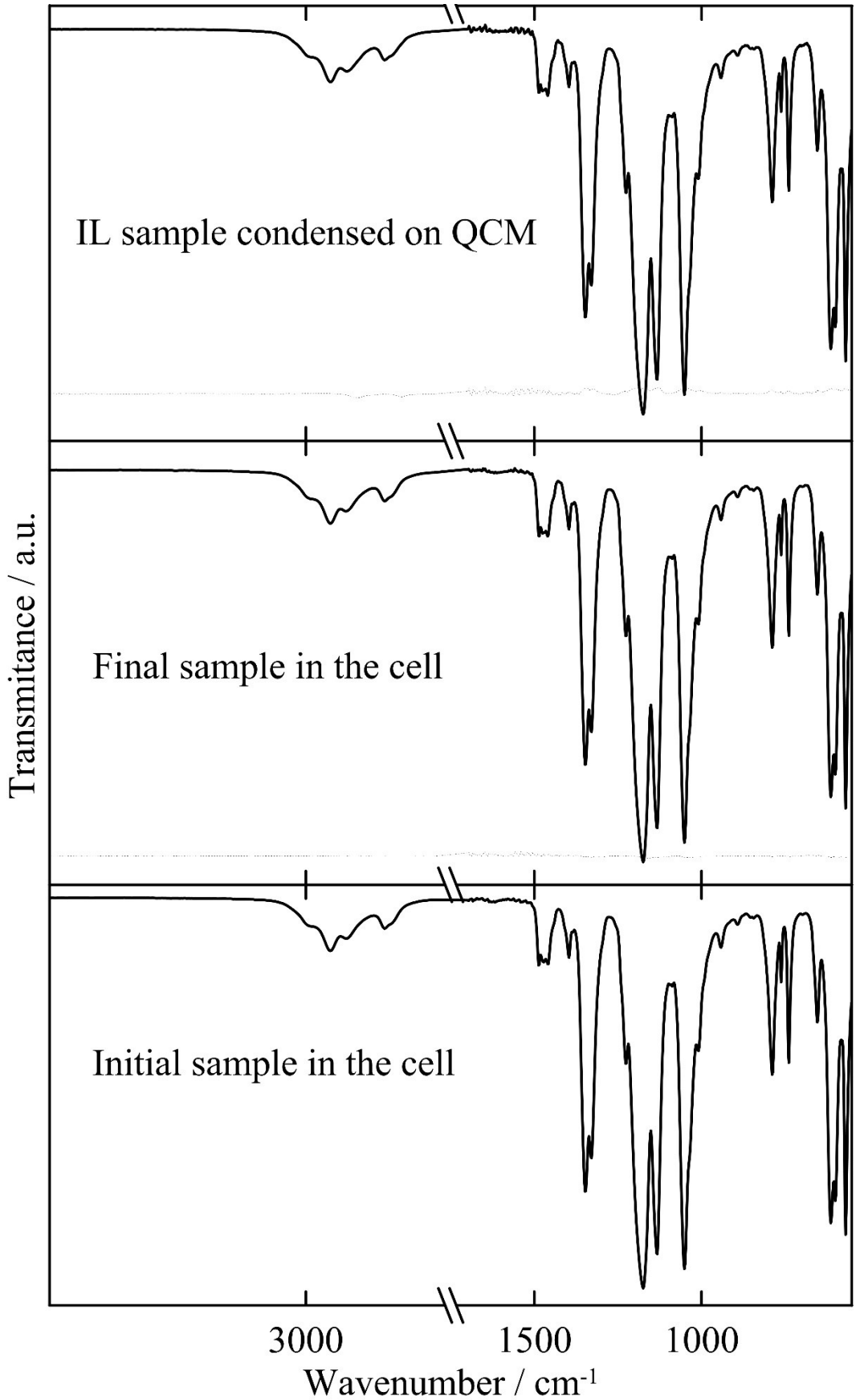

Fig. S4 The spectra of $[N_{2225}][NTf_2]$ studied with QCM technique. Dotted line corresponds to changes in spectra in comparison to initial sample.

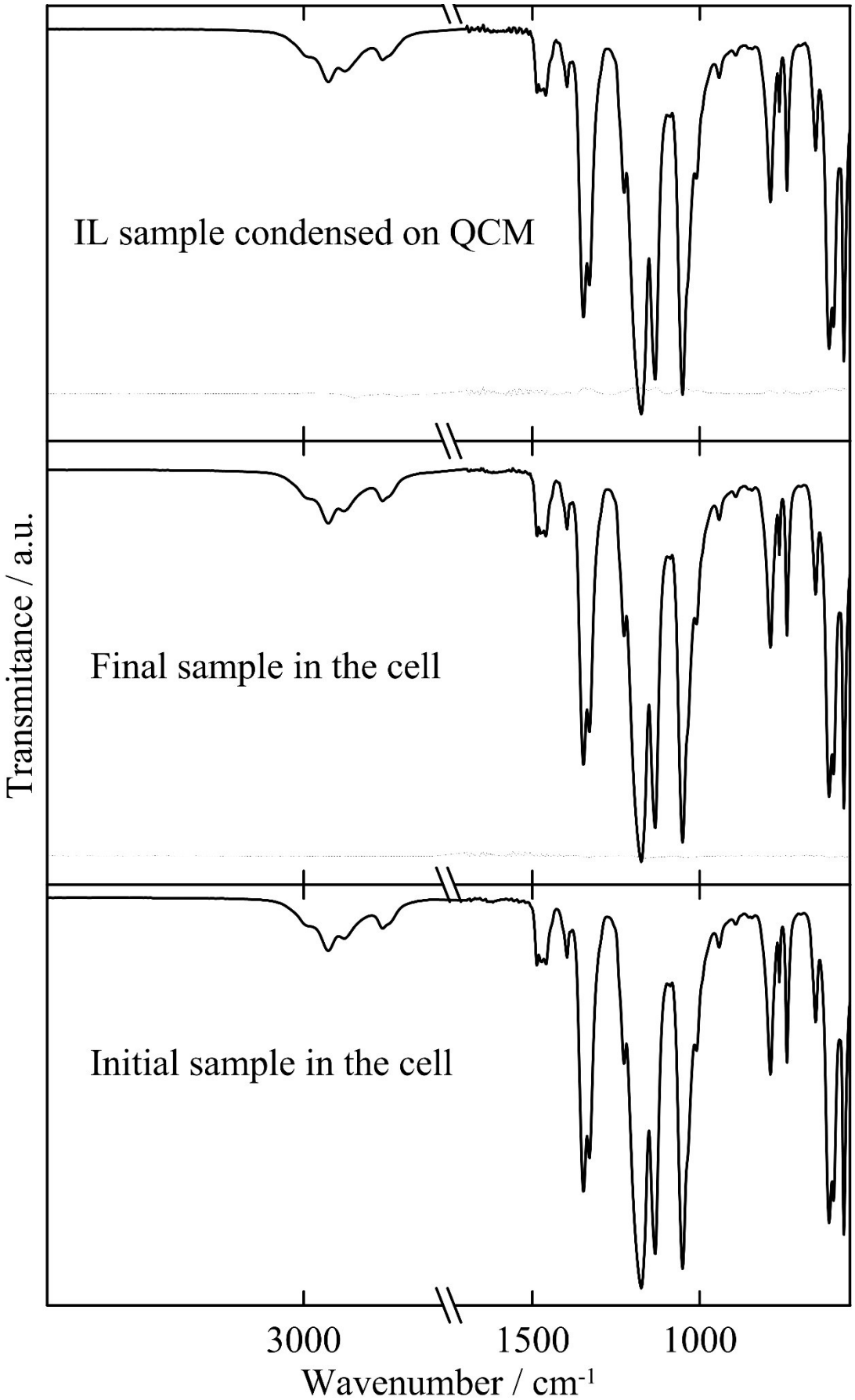

Fig. S5 The spectra of $[N_{2228}][NTf_2]$ studied with QCM technique. Dotted line corresponds to changes in spectra in comparison to initial sample.

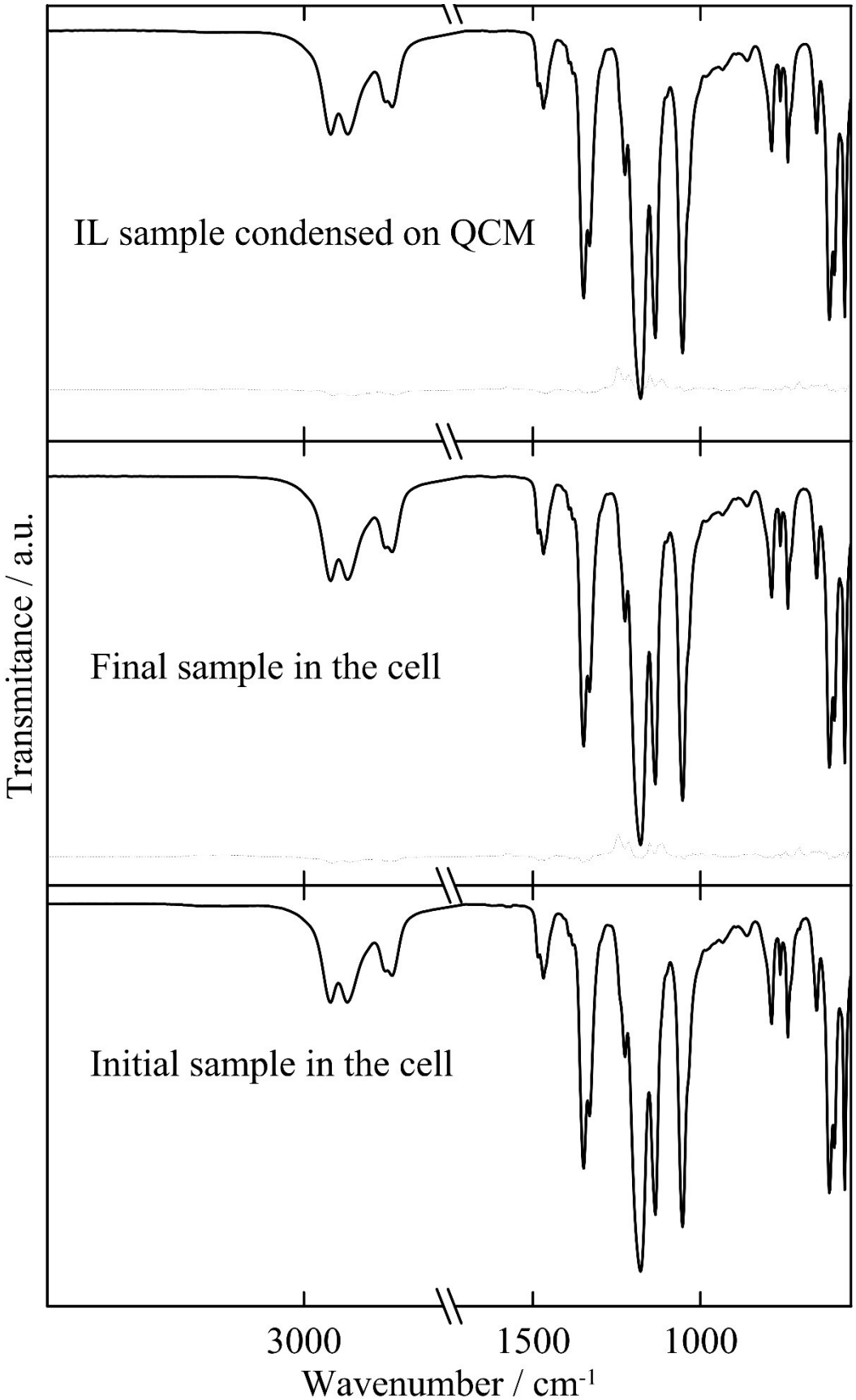

Fig. S6 The spectra of $[N_{2666}][NTf_2]$ studied with QCM technique. Dotted line corresponds to changes in spectra in comparison to initial sample.

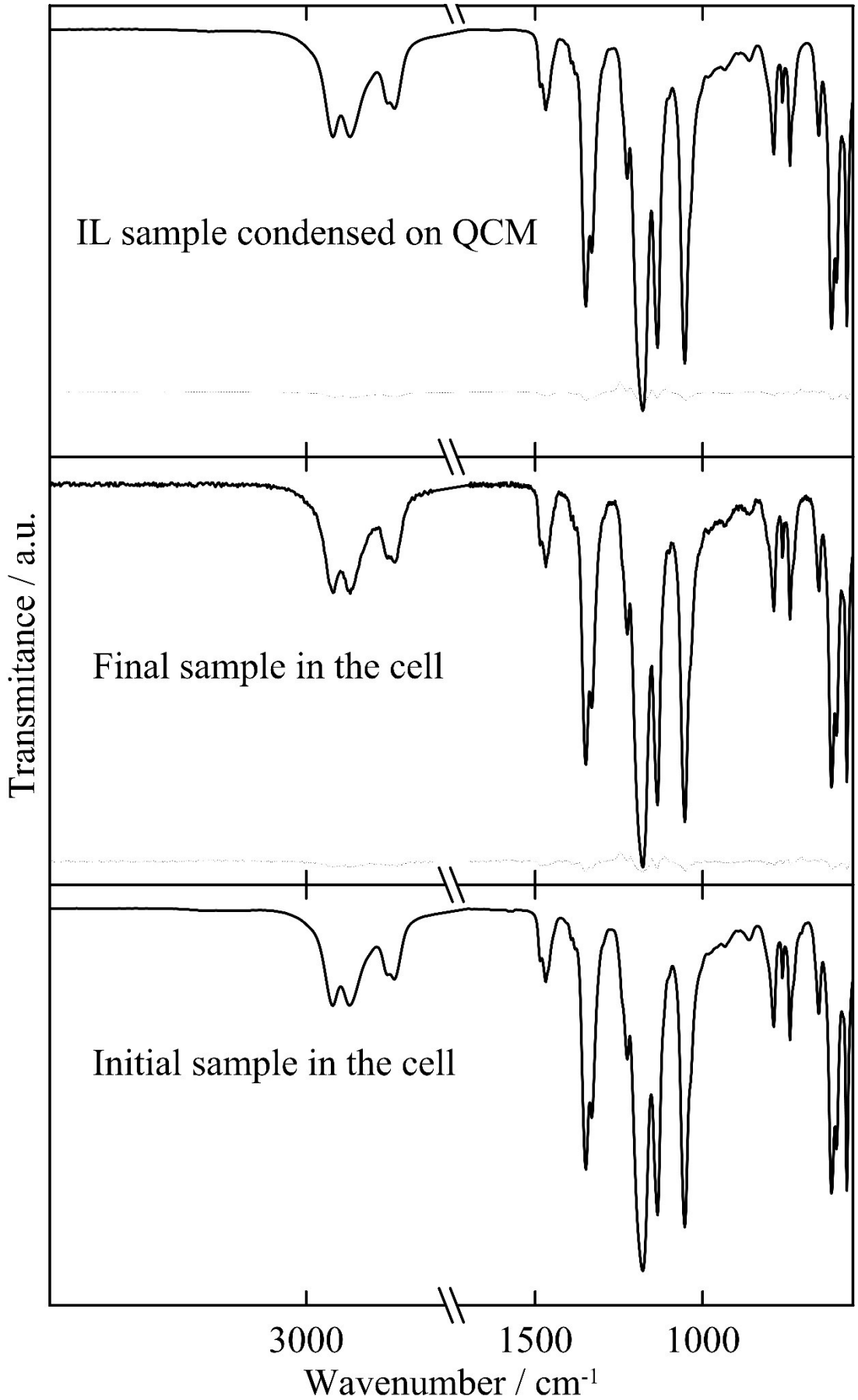

Fig. S7 The spectra of $[N_{6666}][NTf_2]$ studied with QCM technique. Dotted line corresponds to changes in spectra in comparison to initial sample.

Gas-Chromatographic method (GC): The γ_1^{∞} values are related to the total solubility parameter δ_1 for a solute and δ_2 for an IL. In turn, the total solubility parameter (δ_T) at a temperature T is related to vaporization enthalpy over equation:[4]

$$\delta_T = [(\Delta_l^g H_m^o - RT)/V_m]^{0.5} \quad \text{(S5)}$$

where $\Delta_l^g H_m^o$ is the standard molar enthalpy of vaporization (of solute or solvent), R is the ideal gas constant, T is the temperature, and V_m is the molar volume (of solute or solvent). Solubility parameter δ_1 and δ_2 are responsible for a mutual miscibility of a solute and an IL. Quantitatively it is represented over a Flory–Huggins interaction parameters, χ_{12} at infinite dilution:[5]

$$x_{12} = \frac{V_1^*(\delta_1 - \delta_2)^2}{RT} \quad \text{(S6)}$$

where δ_2 is the solubility parameter of the particular IL and δ_1 is the solubility parameter of the solute of interest, R denotes the universal gas constant, T is the temperature, V_1^* is the molar volume of the solute. After a simple algebraic rearrangement of Eq. S6 it gives the following equation:[5]

$$\frac{\delta_1^2}{RT} - \frac{\chi_{12}}{V_1^*} = \left(\frac{2\delta_2}{RT}\right)\delta_1 - \frac{\delta_2^2}{RT} \quad \text{(S7)}$$

The Flory−Huggins interaction parameter χ_{12} at infinite dilution can be derived from experimental activity coefficient at infinite dilution γ_1^{∞} according to Eq. S8:

$$x_{12} = \ln\left(\frac{273.15\,\gamma_1^{\infty} M_2}{TM_1}\right) - \left(1 - \frac{V_1^*}{V_2^*}\right) + \ln\left(\frac{\rho_1}{\rho_2}\right) \quad \text{(S8)}$$

where M_1 and M_2 are the molecular weight of solute and solvent, V_1^* and V_2^* and ρ_1 and ρ_2 are the molar volume and density of solute and solvent, respectively. From a graphical representation of Eq. S7, it is apparent: when the left side of Eq. 9 is plotted against δ_1, the expression $2\delta_2/(RT)$ is the slope of the line and the expression $-\delta_2^2/(RT)$ is the intercept. Using linear regression of the experimental γ_1^{∞}-values, the slope and intercept can be used to determine the solubility parameter of an ionic liquid δ_2. Consequently, the vaporization enthalpy, $\Delta_l^g H_m^o$(298.15 K) of an IL under study can be calculated using Eq. 5 and the δ_2-value as follows:

$$\Delta_l^g H_m^o(T) = [\delta_{2\times} V_m + RT] \quad \text{(S9)}$$

where all values, including V_m are referenced to an arbitrary temperature T, which is 298.15 K in this work.

We fitted Eq. S7 with γ_1^∞-values from Refs.[6–10] [G1-G5]. Tables S5 identify the solutes and the solvents used to obtain δ_2. The δ_2-values were estimated as the average obtained from the slope and the intercept of Eq. 7. Values $\Delta_l^g H_m^o$(298.15 K) were calculated from δ_2 according to Eq. S9. These results are summarized in Table 2.

Table S2 Data[6] used for regression with Eq. (S7) for [N1114][NTf_2]: solubility parameters δ_1 (at 298.15 K) of different solutes and the left part of Eq. (S7).

solute	δ_1 [a]/MPa$^{0.5}$	Y [b]
nonane	15.7	0.0758
decane	15.8	0.0772
undecane	15.9	0.0789
dodecane	16.1	0.0804
methanol	29.4	0.3105
ethanol	26.1	0.249
1-propanol	24.5	0.2203
1-butanol	23.3	0.2009
1-pentanol	22.4	0.1845
1-hexanol	21.7	0.1732

[a] Calculated according to Eq. 11 using vaporisation enthalpies from compilation [11].
[b] The left part of Eq. (S7): $Y = (\delta_1)^2/(RT) - \chi_{12}/V_1$

Table S3 Data[7] used for regression with Eq. (S7) for [N1116][NTf_2]: solubility parameters δ_1 (at 298.15 K) of different solutes and the left part of Eq. (S7).

solute	δ_1 [a]/MPa$^{0.5}$	Y [b]
heptane	15,2	0,0734
octane	15,4	0,0764
nonane	15,7	0,079
decane	15,8	0,0809
undecane	15,9	0,0825
dodecane	16,1	0,0845
tridecane	16,2	0,0853
tetradecane	16,3	0,0868
methanol	29,4	0,311
ethanol	26,1	0,2522
1-propanol	24,5	0,2208
2-propanol	23,6	0,2065
2-methyl-1-propanol	22,9	0,1945
1-butanol	23,3	0,2022

[a] Calculated according to Eq. 11 using vaporisation enthalpies from compilation.[11]
[b] The left part of Eq. (S7): $Y = (\delta_1)^2/(RT) - \chi_{12}/V_1$

Table S4 Data[8] used for regression with Eq. (S7) for [N1118][NTf_2]: solubility parameters δ_1 (at 298.15 K) of different solutes and the left part of Eq. (S7).

solute	δ_1 [a]/MPa$^{0.5}$	Y [b]
heptane	15.2	0.0762
octane	15.4	0.0794
nonane	15.7	0.0822
decane	15.8	0.0842
undecane	15.9	0.0857
dodecane	16.1	0.0878
methanol	29.4	0.3175
ethanol	26.1	0.2488
1-propanol	24.5	0.2214
2-propanol	23.6	0.2063
2-methyl-1-propanol	22.9	0.1954
1-butanol	23.3	0.2028

[a] Calculated according to Eq. S9 using vaporisation enthalpies from compilation.[11]
[b] The left part of Eq. (S7): $Y = (\delta_1)^2/(RT) - \chi_{12}/V_1$

Table S5 Data[8] used for regression with Eq. (S7) for [N111,10][NTf_2]: solubility parameters δ_1 (at 298.15 K) of different solutes and the left part of Eq. (S7).

solute	δ_1 [a]/MPa$^{0.5}$	Y [b]
hexane	14.9	0.0754
heptane	15.2	0.0795
octane	15.4	0.0829
nonane	15.7	0.0861
decane	15.8	0.0879
undecane	15.9	0.0897
dodecane	16.1	0.0917
methanol	29.4	0.3142
ethanol	26.1	0.2499
1-propanol	24.5	0.2222
2-propanol	23.6	0.2078
2-methyl-1-propanol	22.9	0.1965
1-butanol	23.3	0.2041

[a] Calculated according to Eq. S9 using vaporisation enthalpies from compilation.[11]
[b] The left part of Eq. (S7): $Y = (\delta_1)^2/(RT) - \chi_{12}/V_1$

Table S6 Data[8] used for regression with Eq. (S7) for [N1444][NTf_2]: solubility parameters δ_1 (at 298.15 K) of different solutes and the left part of Eq. (S7).

solute	δ_1 [a]/MPa$^{0.5}$	Y [b]
heptane	15.2	0.0761
octane	15.4	0.0795
nonane	15.7	0.0824
decane	15.8	0.0844
undecane	15.9	0.0861
dodecane	16.1	0.0882
methanol	29.4	0.3093

ethanol	26.1	0.2474
1-propanol	24.5	0.2205
2-propanol	23.6	0.2057
2-methyl-1-propanol	22.9	0.1953
1-butanol	23.3	0.2023

[a] Calculated according to Eq. S9 using vaporisation enthalpies from compilation.[11]
[b] The left part of Eq. (S7): $Y = (\delta_1)^2/(RT) - \chi_{12}/V_1$

Table S7 Data[8] used for regression with Eq. (S7) for [N8888][NTf_2]: solubility parameters δ_1 (at 298.15 K) of different solutes and the left part of Eq. (S7).

solute	δ_1 [a]/MPa$^{0.5}$	Y [b]
hexane	14.9	0.0808
heptane	15.2	0.0851
octane	15.4	0.0885
nonane	15.7	0.0914
decane	15.8	0.0934
undecane	15.9	0.0954
dodecane	16.1	0.0977
2-propanol	23.6	0.2024

[a] Calculated according to Eq. S9 using vaporisation enthalpies from compilation.[11]
[b] The left part of Eq. (S7): $Y = (\delta_1)^2/(RT) - \chi_{12}/V_1$

Table S8 Data[9] used for regression with Eq. (S7) for [N2228][NTf_2]: solubility parameters δ_1 (at 298.15 K) of different solutes and the left part of Eq. (S7).

solute	δ_1 [a]/MPa$^{0.5}$	Y [b]
heptane	15.2	0.0781
octane	15.4	0.0815
nonane	15.7	0.085
decane	15.8	0.0864
methanol	29.4	0.3048
ethanol	26.1	0.2478
1-propanol	24.5	0.2215
2-propanol	23.6	0.2065
1-butanol	23.3	0.2036
2-butanol	22.7	0.1932
2-methyl-1-propanol	22.9	0.1949
Tert-butanol	21.7	0.1781
1-pentanol	22.4	0.1897
1-hexanol	21.7	0.1768
Tert-pentanol	21.0	0.1664
cyclohexanol	23.9	0.2082

[a] Calculated according to Eq. S9 using vaporisation enthalpies from compilation.[11]
[b] The left part of Eq. (S7): $Y = (\delta_1)^2/(RT) - \chi_{12}/V_1$

Table S9 Data[10] used for regression with Eq. (S7) for [N1888][NTf_2]: solubility parameters δ_1 (at 298.15 K) of different solutes and the left part of Eq. (S7).

solute	δ_1 [a]/MPa$^{0.5}$	Y [b]
hexane	14.9	0.0837
heptane	15.2	0.0875
octane	15.4	0.0905
methanol	29.4	0.3095
ethanol	26.1	0.2528
1-propanol	24.5	0.2221

[a] Calculated according to Eq. S9 using vaporisation enthalpies from compilation.[11]

[b] The left part of Eq. (S7): $Y = (\delta_1)^2/(RT) - \chi_{12}/V_1$

Table S10 Results of regression of solubility parameters pf ammonium based ionic liquids with the [NTf_2] according to Eq. (S7), used for calculation vaporization enthalpies according to Eq. S9.

	[N1114]	[N1116]	[N1118]	[N111,10]	[N1444]	[N2228]	[N1888]	[N8888]
slope	20.9	20.6	20.3	19.7	19.8	19.5	19.0	17.4
intercept	21.8	21.2	20.8	20.2	20.5	20.0	19.0	17.7
average	21.4	20.9	20.6	19.9	20.2	19.7	19.0	17.6

Table S11 Quantification of dispersion forces for tetra-alkyl-ammonium-based ILs and alkyl alkyl-imidazoles (in kJ·mol^{-1}).

Compound	Y	$\Delta_l^g H_m^o((CH_2)_n)$	$-E_{disp}((CH_2)_n\ gas)$
[C_2C_1im][NTf_2]	111.9	14.5	0.5
[C_3C_1im][NTf_2]		17.3	2.7
[C_4C_1im][NTf_2]		20.4	4.6
[C_5C_1im][NTf_2]		23.7	6.4
[C_6C_1im][NTf_2]		28.3	6.8
[C_7C_1im][NTf_2]		31.8	8.3
[C_8C_1im][NTf_2]		37.6	7.5
[$C_{10}C_1$im][NTf_2]		45.0	10.1
[$C_{12}C_1$im][NTf_2]		51.9	13.3
[$C_{14}C_1$im][NTf_2]		60.8	14.5
[$C_{16}C_1$im][NTf_2]		69.4	15.6
[$C_{18}C_1$im][NTf_2]		77.0	18.0
C_1im	48.3	7.0	-2.0
C_2im		9.3	0.7
C_3im		12.8	2.2
C_4im		16.5	3.5
C_5im		20.8	4.2
C_6im		24.8	5.3
C_7im		28.5	6.6
C_8im		33.0	7.1
C_9im		37.3	7.8
C_{10}im		41.3	8.7
C_{11}im		45.6	9.5
C_{12}im		49.3	10.8

Table S12 The enthalpies of vaporization for n-alkanes[11]

n in C_nH_{2n+2}	$\Delta_l^g H^o_m$(298.15 K) /kJ·mol^{-1}	*n* in C_nH_{2n+2}	$\Delta_l^g H^o_m$(298.15 K) /kJ·mol^{-1}
5	26.42	19	96.44
6	31.52	20	101.81
7	36.57	21	106.8
8	41.56	22	111.9
9	46.55	23	117
10	51.42	24	121.9
11	56.58	25	126.8
12	61.52	26	131.7
13	66.68	27	135.6
14	71.73	28	141.9
15	76.77	29	147.1
16	81.35	30	152.3
17	86.47	31	157.3
18	91.44		

Table S13 Experimental enthalpies of vaporization of aliphatic trialkyl amines $N(R)_3$.[12]

Compound	N_C [a]	$\Delta_l^g H^o_m$(298.15 K) /kJ·mol^{-1}
$N(CH_3)_3$	3	22.2
$N(C_2H_5)_3$	6	35.0
$N(C_3H_7)_3$	9	47.2
$N(C_4H_9)_3$	12	60.4
$N(C_5H_{11})_3$	15	73.0
$N(C_6H_{13})_3$	18	85.3
$N(C_7H_{15})_3$	21	94.8
$N(C_8H_{17})_3$	24	106.5
$N(C_9H_{19})_3$	36	158.4

[a] N_C is the total of number of carbon atoms in the alkyl chains

Table S14 Experimental enthalpies of vaporization of $[C_n\text{mim}][NTf_2]$.[13]

Ionic Liquids	N_C, [a]	$\Delta_l^g H^o_m$(298.15 K) /kJ·mol^{-1}
$[C_1\text{mim}][NTf_2]$	2	123.3
$[C_2\text{mim}][NTf_2]$	3	123.9
$[C_3\text{mim}][NTf_2]$	4	127.1
$[C_4\text{mim}][NTf_2]$	5	131.2
$[C_5\text{mim}][NTf_2]$	6	134.7
$[C_6\text{mim}][NTf_2]$	7	140.0
$[C_7\text{mim}][NTf_2]$	8	142.1
$[C_8\text{mim}][NTf_2]$	9	148.2
$[C_{10}\text{mim}][NTf_2]$	11	154.4
$[C_{12}\text{mim}][NTf_2]$	13	161.5
$[C_{14}\text{mim}][NTf_2]$	15	171.9
$[C_{16}\text{mim}][NTf_2]$	17	178.8

[C_{18}mim][NTf_2]	19	189.8

[a] N_C is the total of number of carbon atoms in the alkyl chains

Table S15 Experimental enthalpies of vaporization of N-alkyl-imidazoles[14]

Compound	N_C, [a]	$\Delta_l^g H^o_m$(298.15 K) /kJ·mol^{-1}
C_1im		55.3
C_2im		57.6
C_3im		61.1
C_4im		64.8
C_5im		69.1
C_6im		73.1
C_7im		76.8
C_8im		81.3
C_9im		85.6
C_{10}im		89.6
C_{11}im		93.9
C_{12}im		97.6

[a] N_C is the total of number of carbon atoms in the alkyl chains[14]

Table S16 Differences $\Delta(\Delta_l^g H^o_m(298.15\ K))$ between enthalpies of vaporization of tetralkylammonium based ILs with [NTf_2] anion and the vaporization enthalpy of a n-alkane of the comparable chain length.

N_C, [a]	$\Delta(\Delta_l^g H^o_m$(298.15 K)) /kJ·mol^{-1}
4	110.6
7	106.0
10	101.4
13	96.8
16	92.2
19	87.6
22	83.0
25	78.4
37	60.0

[a] N_C is the total of number of carbon atoms in the alkyl chains

DFT protocol for quantification the gas phase dispersion forces in ILs. The contribution of the dispersion interaction in the stability of ammonium-based ionic liquids was evaluated as difference in total energy of the molecules optimized at B3LYP/cc-tzvp level of theory [15,16] with and without D3 dispersion correction from Grimme [17] with Becky Johnson damping [18]. The geometry optimization was carried out with Gaussian16 package.

The main challenging task in theoretical study of molecular or ionic compounds with long side alkyl chains is to correctly establish the conformational ensemble. In the presented study we

applied Conformer Rotamer Ensemble Sampling Tool (CREST) by Grimme [19] utilizing GFN2-xtb method [20,21] for tight optimization of found conformers and evaluation of relative total energy. The complete evaluation of the dispersive energy for whole ensemble of conformers is time and resource consuming. Therefore, to the energies of GFN2-xtb method were used for evaluation of the enthalpy correction of the conformational ensemble at 298.15 K. The closest by energy to the correction conformer was chosen as representative for evaluation of dispersive contribution.

The energy distribution of evaluated with CREST procedure conformational ensembles, the molar fraction of the conformers and corresponding Enthalpy correction for the conformer mixing is presented in Figure S8. The geometries of optimized most relevant conformers are given in Figure S9.

The equilibrium composition was evaluated from the relative energy of the conformers evaluated with GFN2-xtb method assuming that the absolute entropy, zero-point vibration energy (ZPVE) and thermal correction to 298.15 K for all conformers are equal:

$$\mathrm{d}G_i = \mathrm{d}H_i - T\mathrm{d}S_i = \mathrm{d}H_i = \mathrm{d}E_{\mathrm{tot}i} \tag{S10}$$

where $\mathrm{d}G_i$ is the Gibb's energy difference between i^{th} and the most stable conformer, $\mathrm{d}H_i$, $\mathrm{d}S_i$, and $\mathrm{d}E_{\mathrm{tot}i}$ are the corresponding enthalpy, entropy and electronic energy differences, T is the temperature. The molar fraction of each conformer is evaluated according to the protocol of statistical thermodynamics:

$$x_i = \frac{exp\left(^{-\Delta E_{toti}}/_{RT}\right)}{\sum exp\left(^{-\Delta E_{toti}}/_{RT}\right)} \tag{S11}$$

where x_i is the molar fraction of i^{th} conformer in the equilibrium ensemble at temperature T. The enthalpy correction was evaluation as follows:

$$H_{mix} = \sum_i H_i x_i \tag{S12}$$

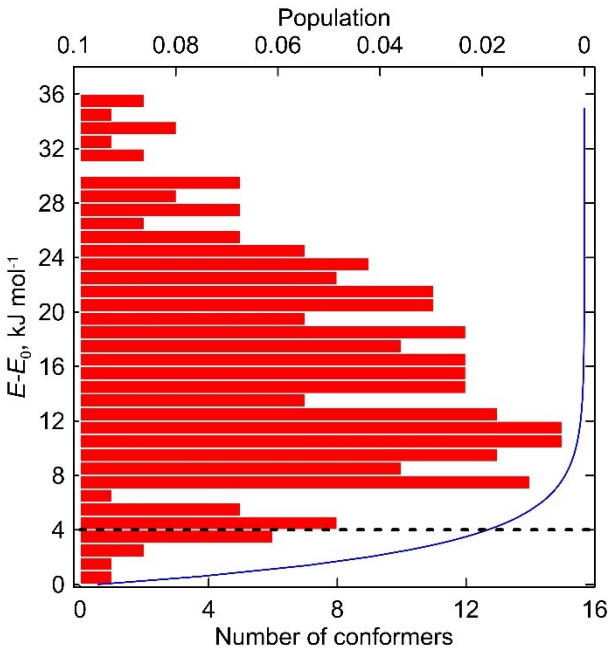

[N1123][NTf2]

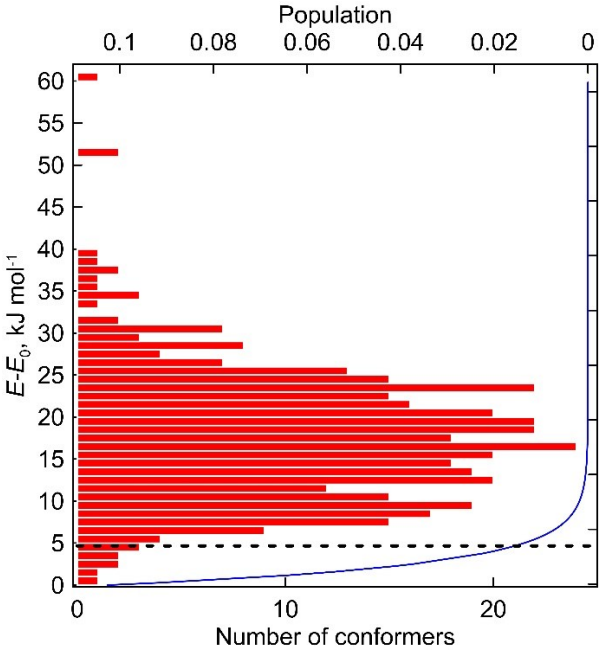

[N1114][NTf2]

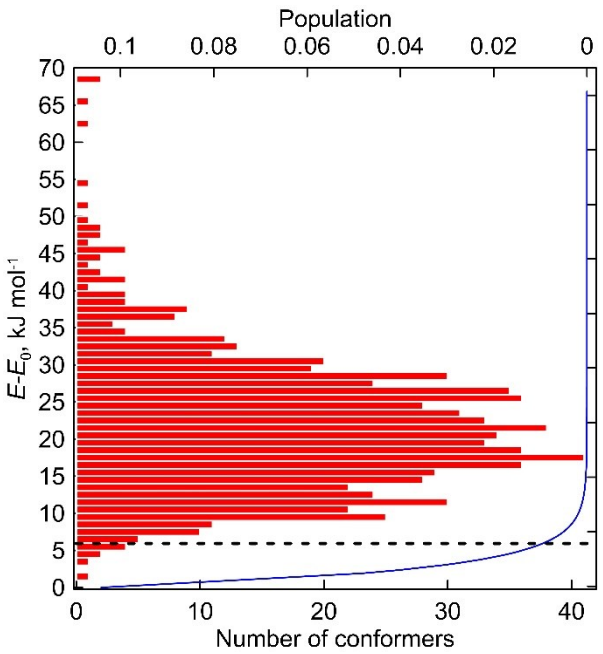

[N1115][NTf2]

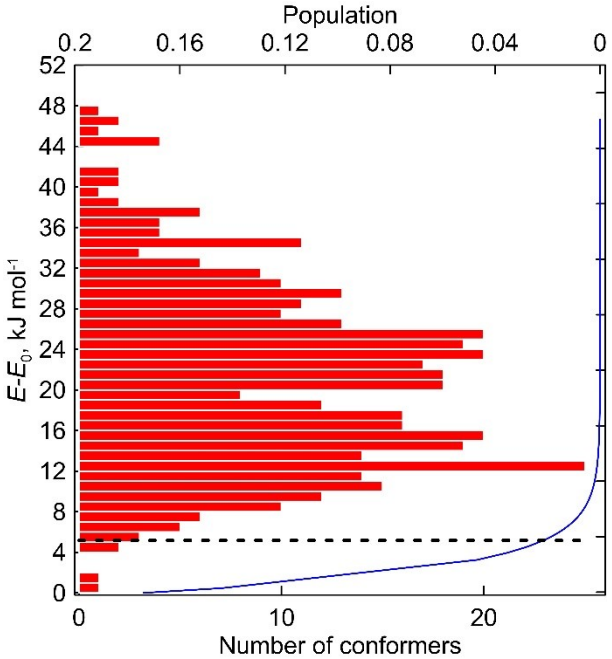

[N1224][NTf2]

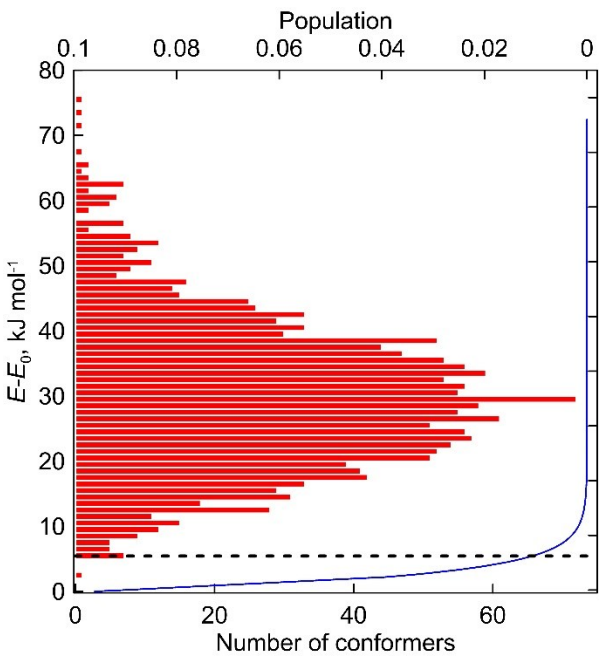

$[N_{2225}][NTf_2]$

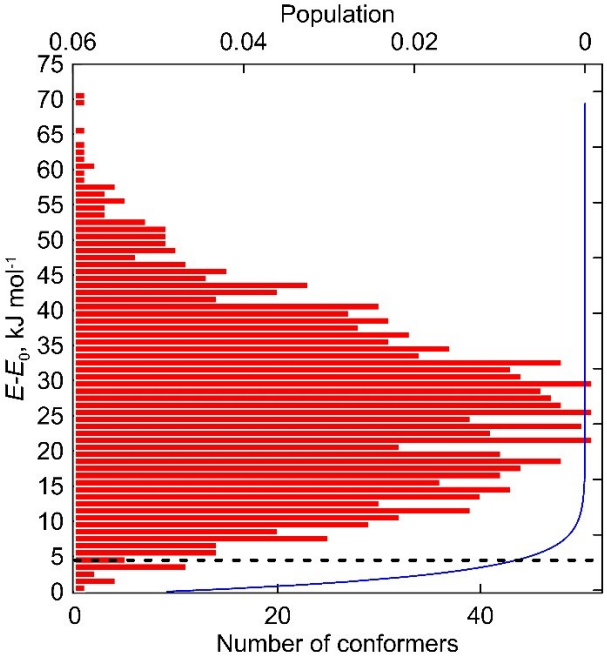

$[N_{1444}][NTf_2]$

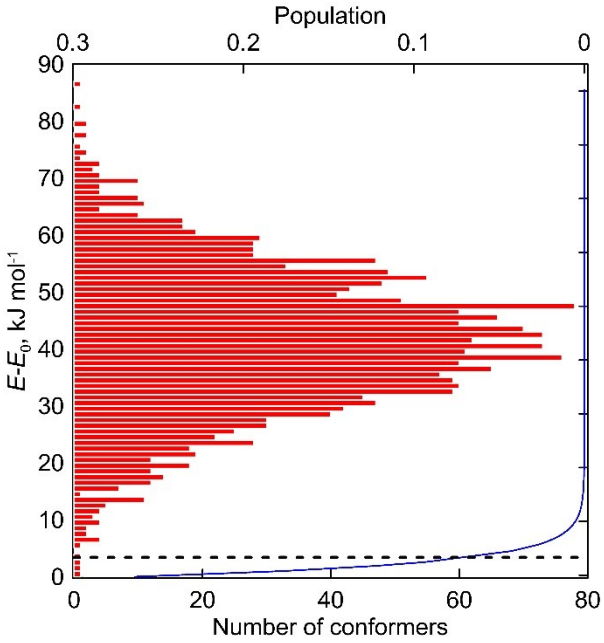

$[N_{2228}][NTf_2]$

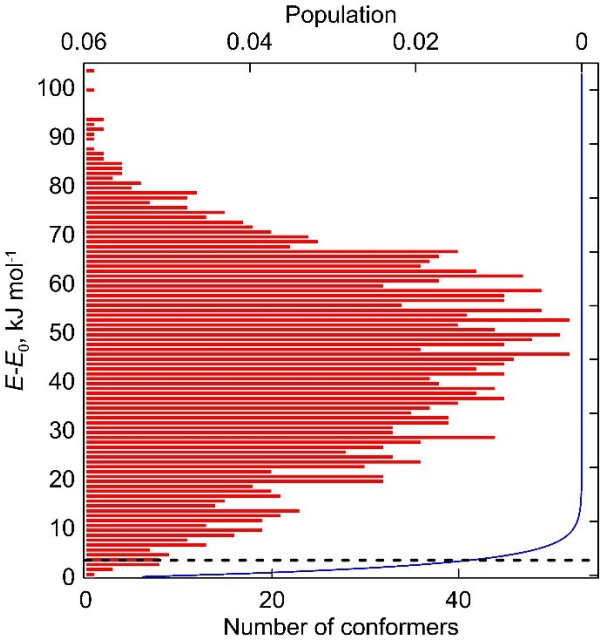

$[N_{2666}][NTf_2]$

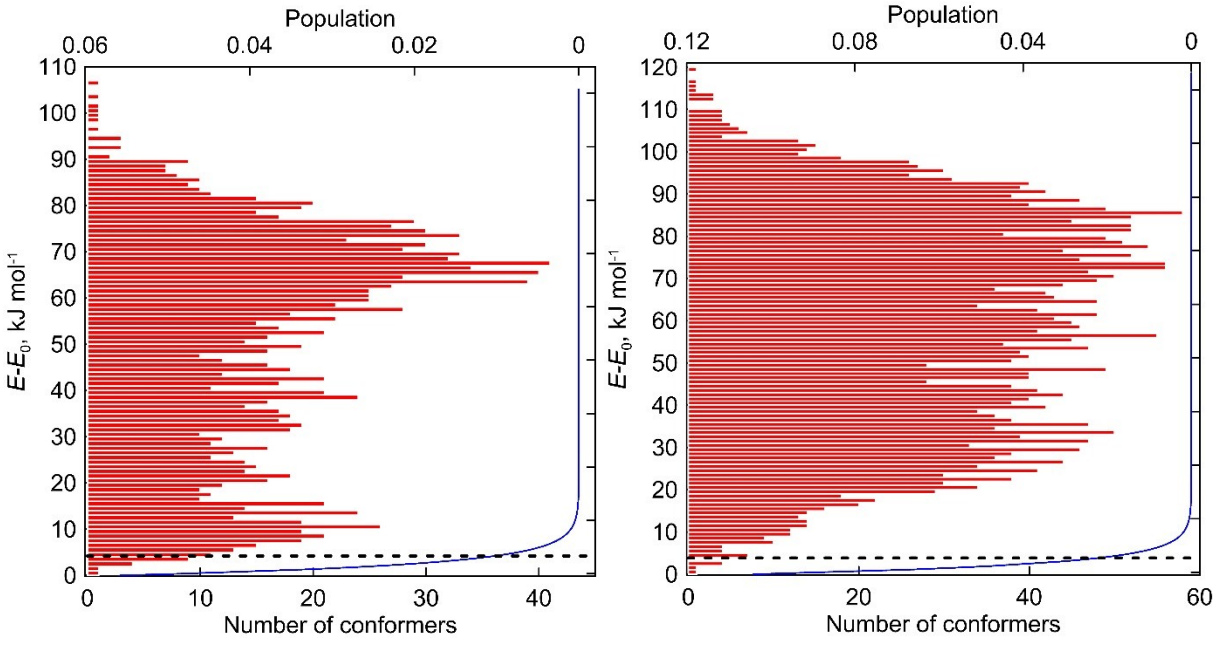

$[N_{6666}][NTf_2]$ $[N_{1888}][NTf_2]$

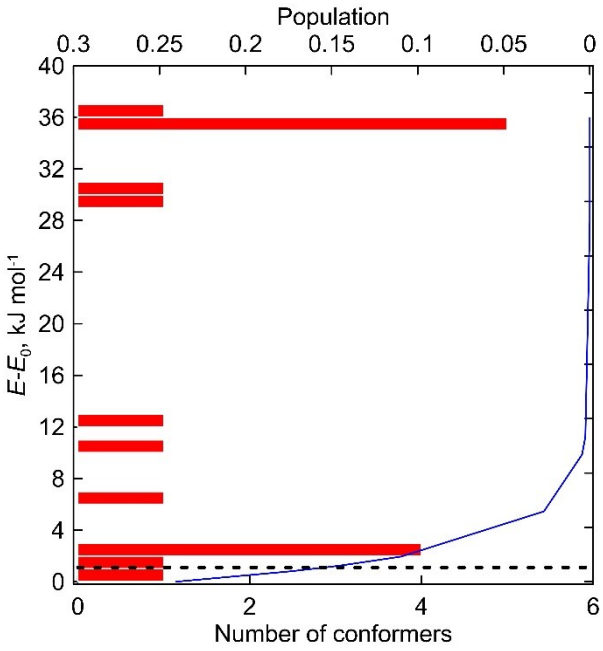

$[NH_4][NTf_2]$

Figure S8. The energy distribution of conformers for studied ILs evaluated by using CREST procedure.[19] Red bars show the number of conformers with corresponding relative energies with 1 kJ·mol^{-1} step. The blue line shows the molar fraction of each conformer in the equilibrium mixture. Black dash line corresponds to enthalpy contribution of conformer mixture.

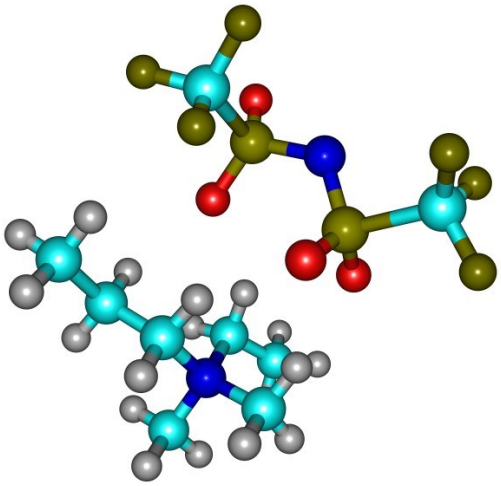

$[N_{1123}][NTf_2]$

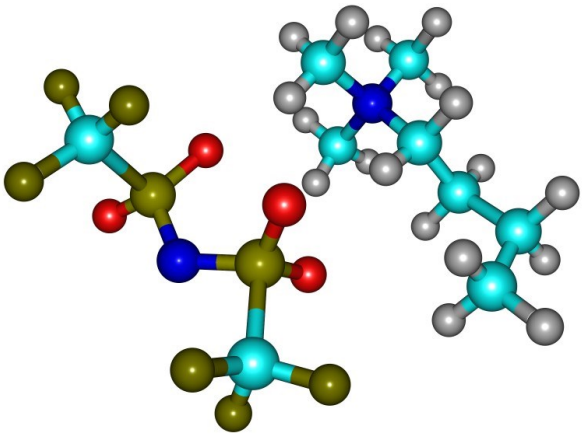

$[N_{1114}][NTf_2]$

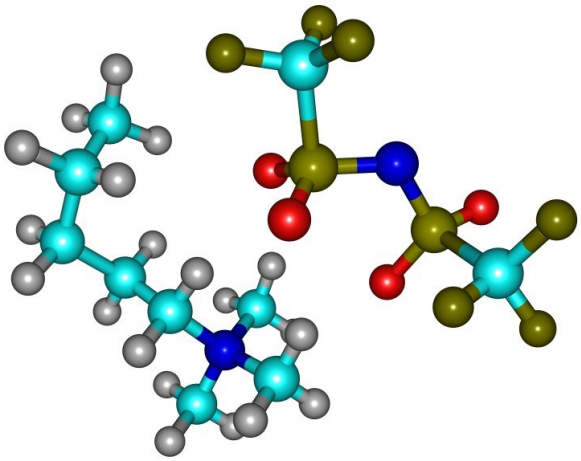

$[N_{1115}][NTf_2]$

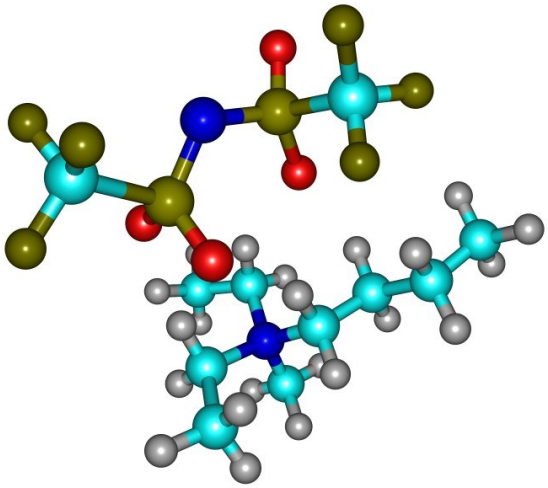

$[N_{1224}][NTf_2]$

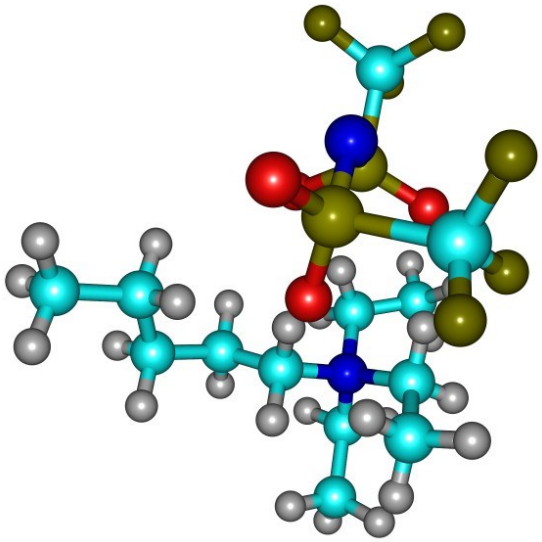

$[N_{2225}][NTf_2]$

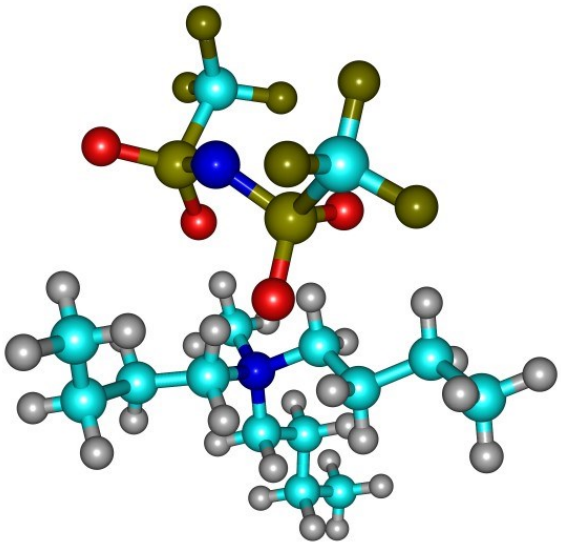

$[N_{1444}][NTf_2]$

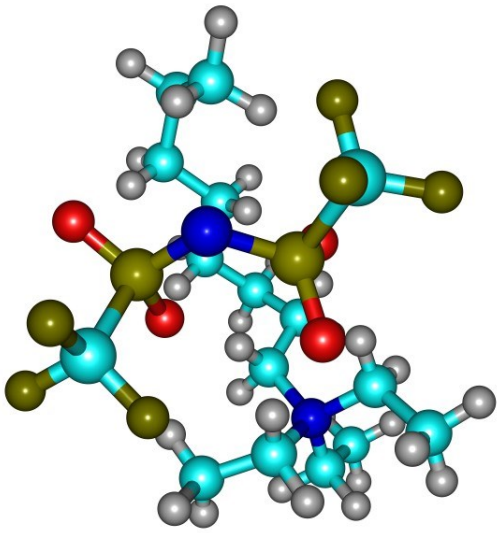

$[N_{2228}][NTf_2]$

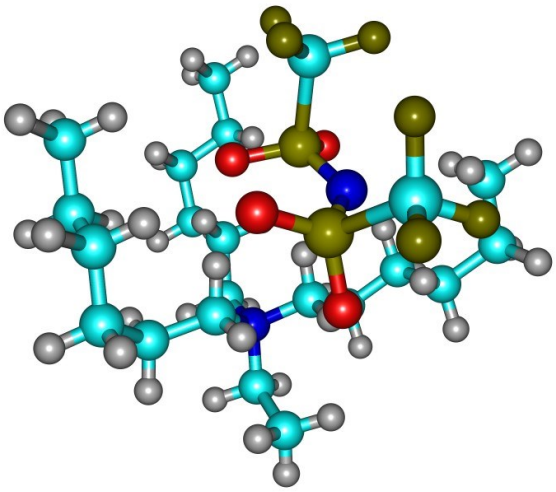

$[N_{2666}][NTf_2]$

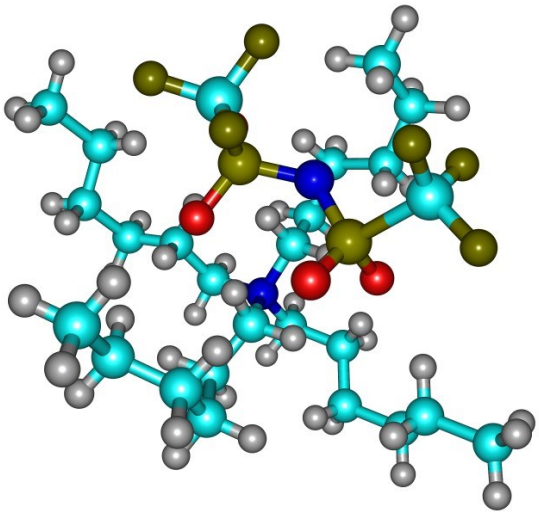

$[N_{6666}][NTf_2]$

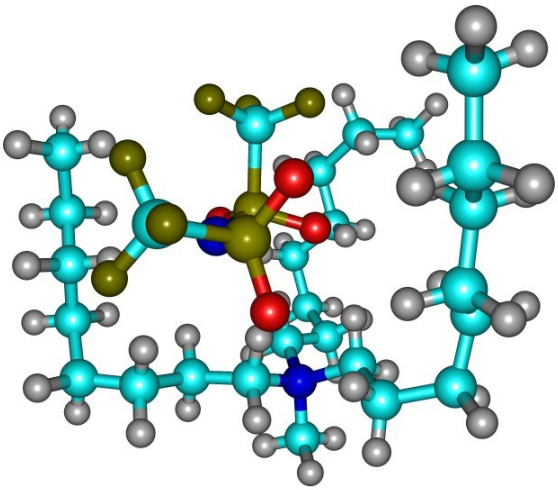

$[N_{1888}][NTf_2]$

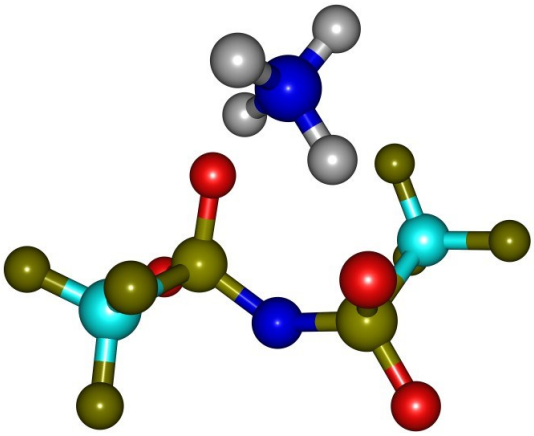

$[NH_4][NTf_2]$

Fig. S9 The geometry of relevant conformers for studied ILs optimized at B3LYP/ cc-tzvp (D3(BJ)) level of theory.

References:

1 S. P. Verevkin, D. H. Zaitsau, V. N. Emel`yanenko and A. Heintz, *J. Phys. Chem. B*, 2011, **115**, 12889–12895.

2 G. Sauerbrey, *Zeitschrift fur Phys.*, 1959, **155**, 206–222.

3 D. H. Zaitsau, A. V Yermalayeu, V. N. Emel'yanenko, S. Butler, T. Schubert and S. P. Verevkin, *J. Phys. Chem. B*, 2016, **120**, 7949–7957.

4 C. M. Hansen, *Prog. Org. Coatings*, 2004, **51**, 77–84.

5 B. Yoo, W. Afzal and J. M. Prausnitz, *Ind. Eng. Chem. Res.*, 2012, **51**, 9913–9917.

6 A. Heintz, T. V Vasiltsova, J. Safarov, E. Bich and S. P. Verevkin, *J. Chem. Eng. Data*, 2006, **51**, 648–655.

7 F. Mutelet, A.-L. Revelli, J.-N. Jaubert, L. M. Sprunger, W. E. Acree Jr. and G. A. Baker, *J. Chem. Eng. Data*, 2010, **55**, 234–242.

8 W. E. Acree, G. A. Baker, F. Mutelet and J.-C. Moise, *J. Chem. & Eng. Data*, 2011, **56**, 3688–3697.

9 M. Wlazło and U. Domańska, *Sep. Purif. Technol.*, 2016, **162**, 162–170.

10 N. V Gwala, N. Deenadayalu, K. Tumba and D. Ramjugernath, *J. Chem. Thermodyn.*, 2010, **42**, 256–261.

11 V. V. Majer, V. V. Svoboda and H. v. Kehiaian, *Enthalpies of vaporization of organic compounds: A critical review and data compilation*, Blackwell Scientific Publications, Oxford, 1985.

12 J. B. Pedley, R. D. Naylor, S. P. Kirby and J. B. Pedley, *Thermochemical data of organic compounds.*, Chapman & Hall, London, 2nd edn., 1986.

13 S. P. Verevkin, D. H. Zaitsau, V. N. Emel'yanenko, A. V Yermalayeu, C. Schick, H. Liu, E. J. Maginn, S. Bulut, I. Krossing and R. Kalb, *J. Phys. Chem. B*, 2013, **117**, 6473–6486.

14 V. N. Emel'yanenko, S. V. Portnova, S. P. Verevkin, A. Skrzypczak and T. Schubert, *J. Chem. Thermodyn.*, 2011, **43**, 1500–1505.

15 D. E. Woon and T. H. Dunning, *J. Chem. Phys.*, 1993, **98**, 1358–1371.

16 K. A. Peterson, D. E. Woon and T. H. Dunning, *J. Chem. Phys.*, 1994, **100**, 7410–7415.

17 S. Grimme, J. Antony, S. Ehrlich and H. Krieg, *J. Chem. Phys.*, 2010, **132**, 154104.

18 S. Grimme, S. Ehrlich and L. Goerigk, *J. Comput. Chem.*, 2011, **32**, 1456–1465.

19 P. Pracht, F. Bohle and S. Grimme, *Phys. Chem. Chem. Phys.*, 2020, **22**, 7169–7192.

20 C. Bannwarth, S. Ehlert and S. Grimme, *J. Chem. Theory Comput.*, 2019, **15**, 1652–1671.

21 P. Pracht, E. Caldeweyher, S. Ehlert and S. Grimme, *ChemRxiv. Prepr.*, , DOI:10.26434/chemrxiv.8326202.v1.